

Enhanced Artificial Neural Network Applications for Spatial Localization Stochastic EM Radiation Sources



Zoran Stankovic¹, Nebojsa Doncov¹, Ivan Milovanovic², Bratislav Milovanovic²

¹Faculty of Electronic Engineering
University of Nis

A. Medvedeva 14, 18000, Nis
zoran.stankovic,nebojsa.doncov@elfak.ni.ac.rs

²Singidunum University, DLS center Nis, 18000 Nis
ivanshix@gmail.com, batam@pogled.net

ABSTRACT: *To ensure the enhanced artificial neural network applications for spatial localization stochastic EM radiation sources, we present a system with results. We have given the stochastic sources near field representation with antenna arrays and dipole elements. Besides, the correlation matrix calculation architecture is presented. It will help to develop neural models for the 1D and 2D DoA estimation. In addition, we have presented the environment when sources are moving towards one direction and their corresponding position is decided by one protrusion angle with linear antenna. We have supported the illustrations with neural model capability to the issues of the DoA calculation for the sources.*

Keywords: Source Localization, Stochastic Radiation, Moveable Sources, Correlation Matrix, Neural Networks

Received: 19 November 2021, Revised 3 February 2022, Accepted 23 February 2022

DOI: 10.6025/jism/2022/12/2/27-44

Copyright: with Authors

1. Introduction

Today, there are many techniques aiming to improve the performances of different wireless communication systems. One of them is a technique based on antenna arrays with adaptive beamforming capabilities [1,2]. It offers possibilities to minimize or even eliminate interferences and to enhance information signals at the reception by using antennas with radiation pattern optimized from the knowledge of interference sources positions. Location of unwanted signal sources are usually determined by employing some of the available DoA (Direction of Arrival) estimation algorithms, e.g. MUSIC [1-3]. These algorithms are usually very accurate but majority of them require complex and hardware- and timeconsuming mathematical operations which limit their applications in real working environment. One possible alternative to these algorithms is based on using artificial neural networks (ANNs) [4-16]. They provide the DoA estimation of almost same precision as e.g. MUSIC but with much faster run-time due to avoidance of exhausting calculations.

Authors of this paper have considered in the past the application of ANNs for the one dimensional (1D) and twodimensional (2D) DoA estimation of deterministic electromagnetic (EM) radiation sources [4-6]. Stochastic EM sources have to be also considered from the interference point of view [17,18] and their angular positions have been determined by using the ANN models developed by the authors of this paper in [7-14]. In [7-12], authors have proposed the neural model for the 1D DoA estimation of moving stochastic sources whose locations were characterized only by one angular coordinate (azimuth). In [7-9] neural models for the DoA estimation of either single or multiple uncorrelated stochastic sources were developed while in [10] an enhancement of these models was done in order to be able to first determine the number of sources present in the monitoring space and then perform the DoA estimation. In [11-12] neural models for 1D DoA estimation of stochastic sources, which are mutually partially correlated, were proposed. Also in [13,14] neural models for 2D DoA estimation were developed. In [13], the model was applied to determine two angular spatial coordinates of one stochastic source, and in [14] for determining angular coordinates of two uncorrelated stochastic sources moving in 2D space (plane).

2. Stochastic Source Location Based on 1D DOAANN Modeling

2.1. Correlation Matrix Calculation for 1D Source Movement

In [17,18], a stochastic source was modelled by a uniform antenna array with N dipole elements at mutual distance equal to the half of the operating wavelength (Figure 1). The level of correlation between dipoles feed currents $I = [I_1, I_2, \dots, I_N]$, $c^I(\omega)$, describing the noisy source radiation, is of the form [17,18]:

$$c^I(\omega) = \lim_{T \rightarrow \infty} \frac{1}{2T} [I(\omega)I(\omega)^H] \quad (1)$$

To find the total electric field in the far-field sampling point, vector \mathbf{M} , comprising the contribution of each antenna array element with radiation pattern $F(\theta)$, is needed:

$$\mathbf{M}(\theta) = jz_0 \frac{F(\theta)}{2\pi r} \begin{bmatrix} \frac{e^{jkr_1}}{r_1} & \frac{e^{jkr_2}}{r_2} & \dots & \frac{e^{jkr_N}}{r_N} \end{bmatrix} \quad (2)$$

$$E(\theta) = \mathbf{M}(\theta)\mathbf{I} \quad (3)$$

where z_0 and k are free-space impedance and phase constant, respectively, r_1, r_2, \dots, r_N are the distances between the farfield sampling point and antenna array elements and $E(\theta)$ is the total electric field intensity in sampling point in far-field positioned at angle θ in azimuth plane with the respect to the first element of antenna array. If there are M sampling points in the far-field, then notation $r_{i,m}$, representing the distance between i -th element ($1 \leq i \leq N$) in the antenna array and m -th sampling point in the far-field ($1 \leq m \leq M$) (see Figure 1), can be used. Position of these points (Y_1, Y_2, \dots, Y_M) in the far-field, is described by the azimuth plane angles $(\theta_1), (\theta), \dots, (\theta_M)$, determined as previously said with the respect to the first element of antenna array. The correlation matrix of signals sampled at these points can be calculated as:

$$C_E[i, j] = \mathbf{M}(\theta_i)c^I\mathbf{M}(\theta_j)^H \quad (4)$$

$i = 1, \dots, M \quad j = 1, \dots, M$

For the multiple stochastic sources in the azimuth plane, the level of EM field and the elements of correlation matrix C_E in particular far-field sampling point, are calculated by the superposition of radiation field from all sources. If there are S stochastic sources, then the vector \mathbf{M} has a form [8]:

$$\mathbf{M}(\theta) = jz_0 \frac{F(\theta)}{2\pi} \cdot \begin{bmatrix} \frac{e^{jkr_1^{(1)}}}{r_1^{(1)}} \dots \frac{e^{jkr_N^{(1)}}}{r_N^{(1)}} & \frac{e^{jkr_1^{(2)}}}{r_1^{(2)}} \dots \frac{e^{jkr_N^{(2)}}}{r_N^{(2)}} & \dots & \frac{e^{jkr_1^{(S)}}}{r_1^{(S)}} \dots \frac{e^{jkr_N^{(S)}}}{r_N^{(S)}} \end{bmatrix} \quad (5)$$

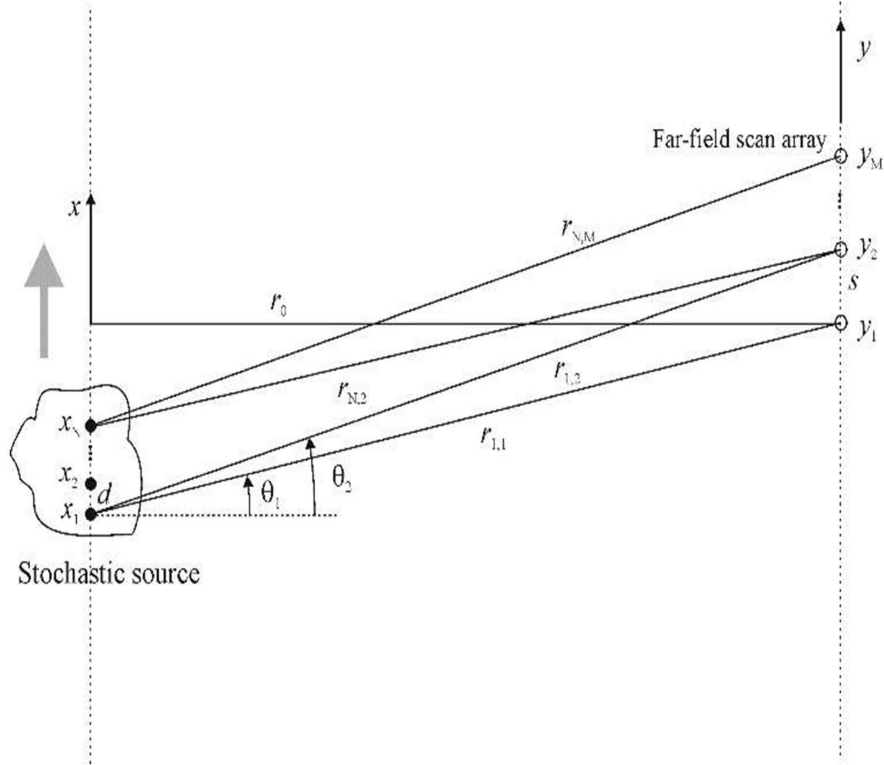


Figure 1. The position of stochastic source in azimuth plane with respect to the location of EM field sampling points in the far-field scan area [8]

where $r_i^{(j)}$ is the distance between i -th element in antenna array, representing j -th stochastic source, and the sampling point in far-field, while the feed currents vector is:

$$\mathbf{I} = [I_1^{(1)} \dots I_N^{(1)} I_1^{(2)} \dots I_N^{(2)} \dots I_1^{(S)} \dots I_N^{(S)}] \quad (6)$$

where $I_i^{(j)}$ is the feed current of i -th element in antenna array representing j -th stochastic source [8].

By using Eqs.(3-6), the EM field in the sampling point in the far-field, as well as the elements of correlation matrix C_E can be obtained. In addition, if unknown, matrix $c^l(\omega)$ can be determined by measuring the electric field in the nearfield of stochastic source [8].

2.2. Neural model for 1D DoA estimation

The Neural model, based on MLP ANN, is trained to extract information about position of S stochastic sources in azimuth plane from the correlation matrix C_E [8]:

$$\boldsymbol{\theta} = f(\mathbf{C}_E) \quad (7)$$

In Eq.(7), vector $\boldsymbol{\theta}$ is azimuthal angle vector of stochastic sources, $\boldsymbol{\theta} = [\theta_1, \theta_2, \dots, \theta_S]$, while the elevation coordinates of radiation sources position are in this case neglected. The architecture of developed neural model is shown in Figure 2 and it can be

represented as:

$$\mathbf{y}_l = F(\mathbf{w}_l \mathbf{y}_{l-1} + \mathbf{b}_l) \quad l=1,2 \quad (8)$$

where \mathbf{y}_{l-1} vector describes the output of (l-1)-th hidden layer, \mathbf{w}_l is a connection weight matrix among (l-1)-th and lth hidden layer neurons and \mathbf{b}_l is a vector containing biases of l-th hidden layer neurons [8]. F is the activation function of neurons in hidden layers and in this case it is a hyperbolic tangent sigmoid transfer function:

$$F(u) = \frac{e^u - e^{-u}}{e^u + e^{-u}} \quad (9)$$

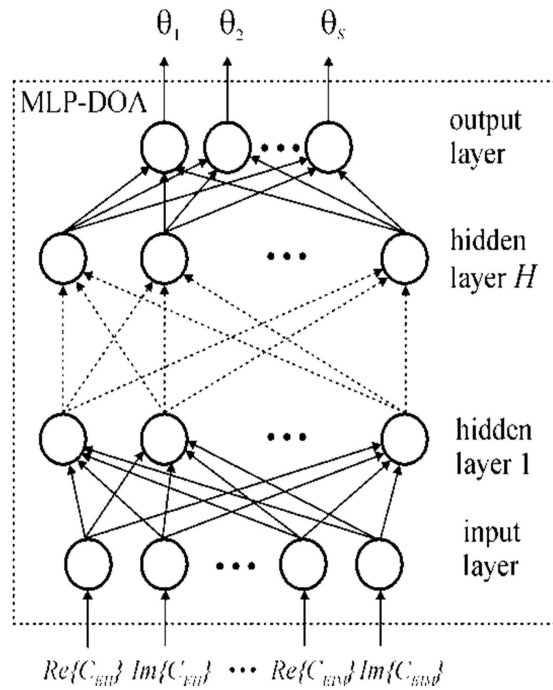


Figure 2. Architecture of MLP neural model for 1D DOA estimation of stochastic EM source signal in azimuth plane [8]

In order to perform mapping it is sufficient to take only the first column of correlation matrix and therefore $\mathbf{y}_0 = [Re\{C_E[1,1]\} \quad Im\{C_E[1,1]\}, \dots, Re\{C_E[1,M]\} \quad Im\{C_E[1,M]\}]$. Also, θ is given as $\theta = \mathbf{w}_3 \mathbf{y}_2$ where \mathbf{w}_3 is a connection weight matrix between neurons of last hidden layer and neurons in output layer [8]. The optimization of weight matrices and biases values during the training allows ANN to approximate the mapping with the wanted accuracy. The general designation for the MLP neural model is $MLPH-N_1 - \dots - N_i - \dots - N_H$ where H is the total number of hidden layers used MLP network, while N_i is the total number of neurons in the i -th hidden layer.

2.3. 1D DoA Estimation - Modelling Results for Uncorrelated Sources

The application of neural model for the 1D DoA estimation of uncorrelated stochastic sources will be illustrated here on the example of two moveable sources ($S=2$). The training of ANN is conducted when there are four equidistant sampling points ($M = 4$) in the far-field scan area, at the mutual distance $d = \lambda/2$, located 100 m from stochastic sources (Table 1) [8]. Angular position in the azimuth plane of two sources at arbitrary angle distance will be determined from the correlation matrix information in the far field scan area. Each of two stochastic sources is described by antenna array with four dipole elements ($N = 4$). The feed currents of four dipole elements are mutually uncorrelated so that \mathbf{c}^l is the unit diagonal matrix. By using Eqs.(4-5) for $N = 4$ and

$M=4$, 861 and 276 uniformly distributed samples are generated for training and testing, respectively, in the range $[-80^\circ 80^\circ]$ at the working frequency of 7.5 GHz. Levenberg- Marquardt method with prescribed accuracy of 10^{-4} is used as a training algorithm. The testing results for six MLP models with the lowest average case error are shown in Table 2, and MLP2-16-8 is chosen as representative neural model.

Frequency	$f = 7.5$ GHz
Number of sources	$S = 2$
Number of antenna array elements per one source	$N = 4$
Sampling points distance from source trajectory	$r_0 = 100$ m
Number of sampling points	$M = 4$
Mutual distance of the sampling points	$s = \lambda/2$ (0.02 m)

Table 1. The Values of Parameters used in Sampling Process [8]

MLP model	WCE [%]	ACE [%]
MLP2-16-8	1.81	0.42
MLP2-14-14	2.26	0.42
MLP2-18-14	2.67	0.39
MLP2-20-10	2.71	0.38
MLP2-16-16	3.27	0.39
MLP2-16-11	3.76	0.41

Table 2. Testing Results for Six MLP Neural Models with the Best Average Errors Statistics [8]

The neural model simulation of testing samples set shows a very good agreement between the output values of neural model and referent azimuth values for two sources (Figure 3 and Figure 4) [8]. In addition, a good agreement with results obtained by MUSIC algorithm can be observed.

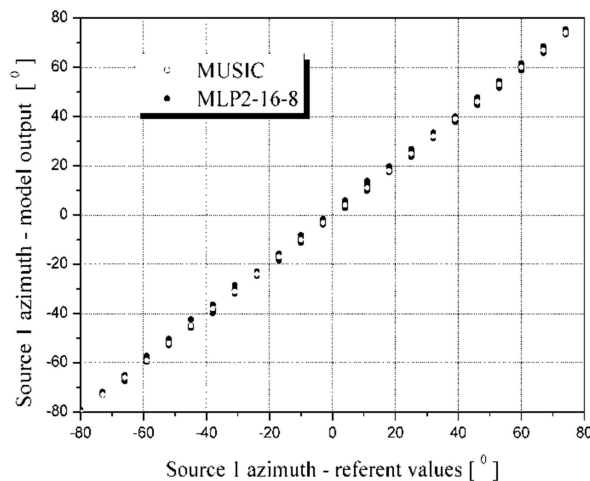


Figure 3. Comparison of MLP2-16-8 model output 1 (azimuth of source 1) with MUSIC and referent azimuth values [8]

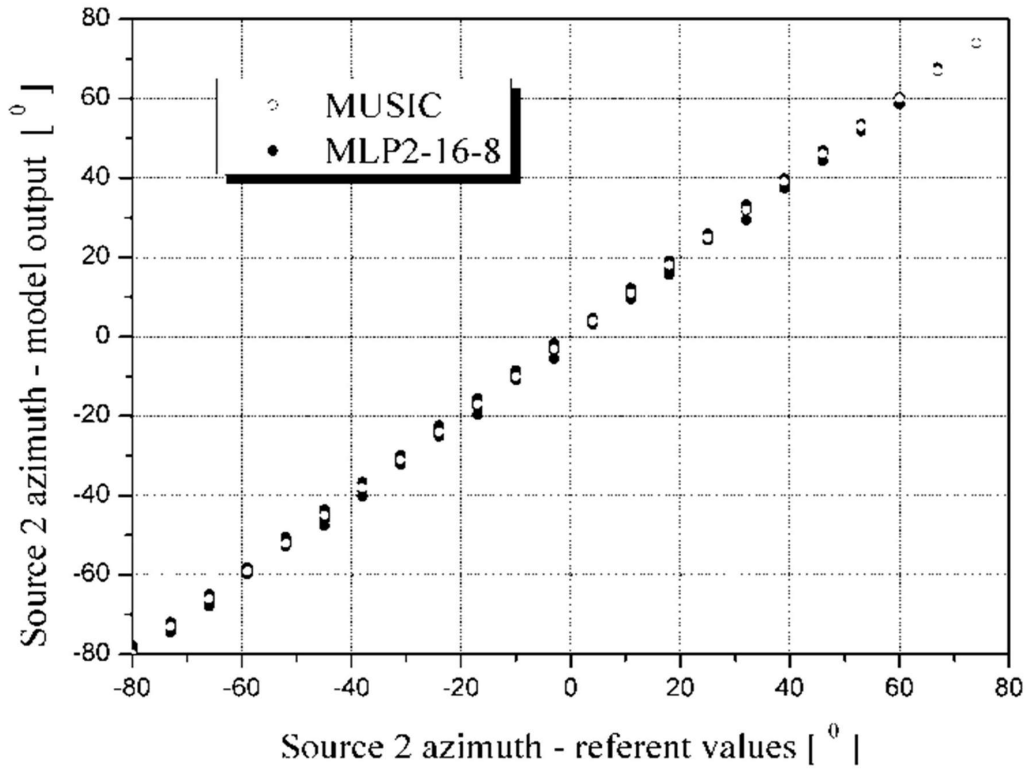


Figure 4. Comparison of MLP2-16-8 model output 2 (azimuth of source 2) with MUSIC and referent azimuth values [8]

2.4. 1D DoA Estimation - Modelling Results for Partially Correlated Sources

MLP neural model, whose architecture was presented in 2.A section, can be also applied for 1D DoA estimation of partially correlated stochastic sources. This capability will be illustrated for two EM sources ($S = 2$) that independently move along linear trajectory distant $r_0 = 100 \text{ m}$ from the antenna array, with whom the signal is sampled at frequency $f = 28 \text{ GHz}$ [11]. Each stochastic source is represented by a dipole ($N = 1$) whose axis is normal on the azimuthal plane.

The scanning width of antenna array in the azimuth is $[-30^\circ 30^\circ]$. Partial correlation between sources is:

$$\mathbf{c}^I = \begin{bmatrix} 1 & c_{12}^I \\ c_{21}^I & 1 \end{bmatrix} \quad (10)$$

where $c = c_{12}^I = c_{21}^I$ is in the range $0.05 \leq c \leq 0.8$ [11]. If sources are uncorrelated then c is equal to zero. For partially correlated and uncorrelated cases we generated separate sample sets for network training and testing, while using common parameters of sampling that are given in Table 3 [11].

For training and testing samples generation we use relations (4) and (5) that establish inverse mapping from that of the MLP DoA model

$$\mathbf{c}_E^I = f_{DoA}^{-1}(\theta_1^I, \theta_2^I, c) \quad (11)$$

Samples for neural network training and testing are given in the format $\{(x^I(\theta_1^I, \theta_2^I, c), \theta_1^I, \theta_2^I)\}$, where x^I is vector of

input model values $\mathbf{x}^t = [Re\{\mathbf{C}_E^t[1,1]\}, \dots, Re\{\mathbf{C}_E^t[1,M]\}, Im\{\mathbf{C}_E^t[1,1]\}, \dots, Im\{\mathbf{C}_E^t[1,M]\}]^T$. For each element of vector x^t we used uniform distribution of samples for azimuth angles of radiation source location and correlation of the form $[\theta_{\min}^t : \theta_{\text{step}}^t : \theta_{\max}^t]$ and $[c_{\min}^t : c_{\text{step}}^t : c_{\max}^t]$, where θ_{\min}^t [°] and c_{\min}^t represent the lowest limit of distribution, θ_{\max}^t [°] and c_{\max}^t represent the highest limit of distribution, while θ_{step}^t and c_{step}^t represent uniform sampling steps [11].

Frequency	$f = 28$ GHz
Number of sources	$S = 2$
Number of antenna array elements per one source	$N = 1$
Sampling points distance from linear source trajectory	$r_0 = 100$ m
Number of sampling antenna array sensors	$M = 6$
Mutual distance of the antenna sensors	$s = \lambda/2$ (5.4 mm)

Table 3. The Values of Parameters used in Sampling Process [11]

For neural model training and testing in the uncorrelated case the following sets were generated [11]:

TRAINING_A set (28920 samples):

$$\left\{ \begin{array}{l} (\mathbf{x}^t(\theta_1^t, \theta_2^t, 0), \theta_1^t, \theta_2^t) | \\ \theta_1^t \in [-30 : 0.25 : 30], \theta_2^t \in [-30 : 0.25 : 30], \theta_1^t > \theta_2^t \end{array} \right\} \quad (12)$$

TEST_A set (5050 samples):

$$\left\{ \begin{array}{l} (\mathbf{x}^t(\theta_1^t, \theta_2^t, 0), \theta_1^t, \theta_2^t) | \\ \theta_1^t \in [-30 : 0.6 : 30], \theta_2^t \in [-30 : 0.6 : 30], \theta_1^t > \theta_2^t \end{array} \right\} \quad (13)$$

For neural model training and testing in the partially correlated case the following sets were generated:

$$\left\{ \begin{array}{l} (\mathbf{x}^t(\theta_1^t, \theta_2^t, c^t), \theta_1^t, \theta_2^t) | \\ \theta_1^t \in [-30 : 1 : 30], \theta_2^t \in [-30 : 1 : 30], \theta_1^t > \theta_2^t, \\ c^t \in [0.05 : 0.05 : 0.8] \end{array} \right\} \quad (14)$$

TRAINING_B set (29280 samples):

$$\left\{ \begin{array}{l} (\mathbf{x}^t(\theta_1^t, \theta_2^t, c^t), \theta_1^t, \theta_2^t) | \\ \theta_1^t \in [-30 : 2.7 : 30], \theta_2^t \in [-30 : 2.7 : 30], \theta_1^t > \theta_2^t, \\ c^t \in [0 : 0.07 : 0.8] \end{array} \right\} \quad (15)$$

TEST_B set (3036 samples):

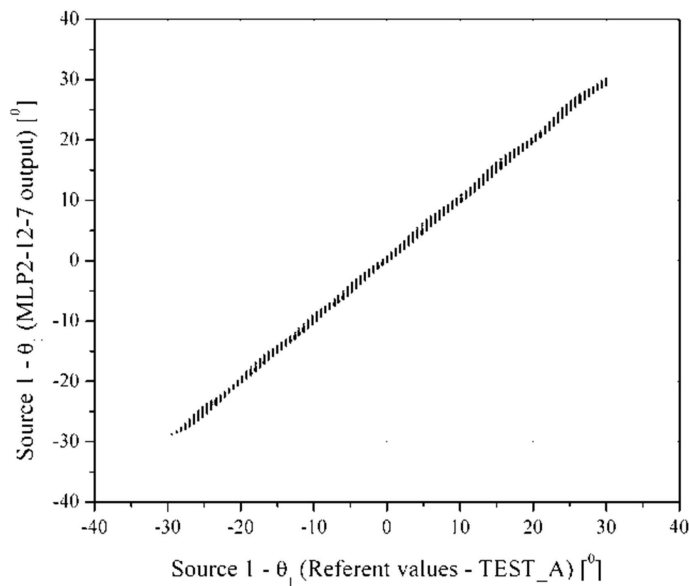
Samples in the TRAINING_A and TEST_A sets were generated under conditions of uncorrelated radiation of two stochastic sources while the samples in the TRAINING_B set are generated under conditions of partial correlation in the range $0.05 \leq c \leq 0.8$. Set TEST_B contains samples that are generated also under variable radiation correlation in above range but also it has samples that are generated under no correlation. Different number of MLP ANNs with two hidden layers ($H = 2$) and different number of neurons in them (MLP2- N_1 - N_2 , $4 \leq N_1, N_2 \leq 23$) were considered during the training, For the testing the values of worst case error (WCE) and average error (ACE) [4,5] were taken into account for model accuracy estimation.

After training the MLP neural models with the set TRAINING_A, the results of the testing of the six models with lowest value of WCE on the set TEST_A are shown in Table IV [11]. Figures. 5(a) and 5(b) [11] present a scattering diagram of MLP2-12-7 model on TEST_A set (this model has shown lowest WCE on that set). It can be seen that all six models show high accuracy in source location estimation. But if in the network input we deliver samples that are generated with some source radiation correlation (set TEST_B) then the models show a high WCE value or high imprecision in source location estimation. That may be seen also in Table IV [11] also from scattering diagram of MLP2-12-7 model on TEST_B set (Figures 6(a) and 6(b)) [11].

MLP model	TEST_A set		TEST_B set	
	WCE [%]	ACE [%]	WCE [%]	ACE [%]
MLP2-12-7	2.25	0.36	60.63	6.76
MLP2-13-13	2.26	0.38	87.81	6.01
MLP2-11-4	2.38	0.37	87.31	7.16
MLP2-16-16	2.43	0.37	59.02	6.07
MLP2-12-12	2.51	0.37	89.37	7.17
MLP2-12-5	2.55	0.37	83.99	6.91

Table 4. Testing Results for Six MLP Neural Models Trained on Training_A Set with the Best Average Errors Statistics [11]

After training MLP neural models on the set TRAINING_B, the results from testing of six models with lowest value for WCE on set TEST_B are shown in Table V [11]. In Figs. 7(a) and 7(b) [11] we may see scattering diagram of the MLP2-22-22 model on the set TEST_B (this model has shown lowest value of WCE on that set). It can be seen that the model MLP2-22-22 has a satisfactory accuracy in angle position determination when we use samples for different partial correlations of sources.



(a)

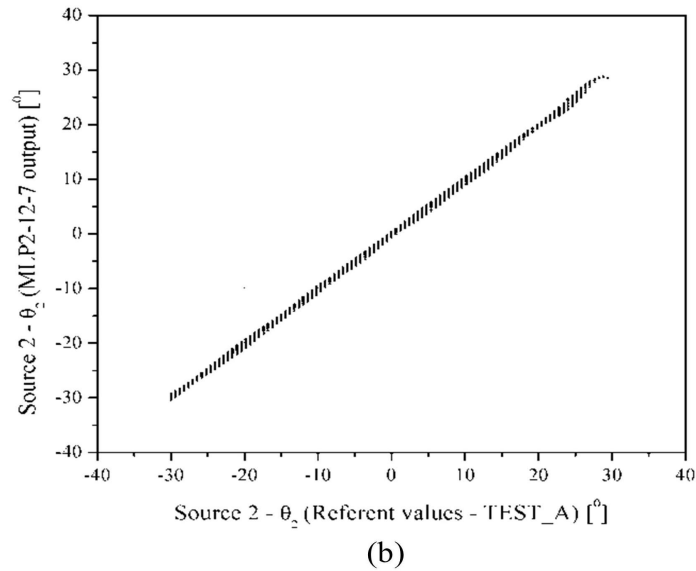
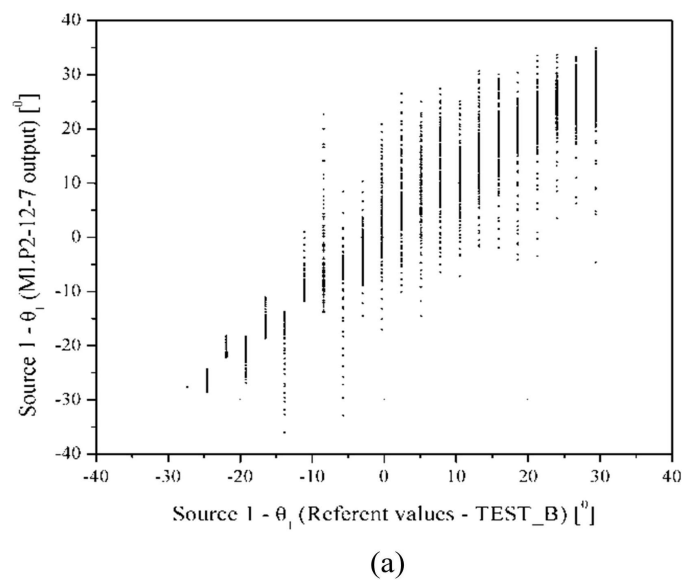
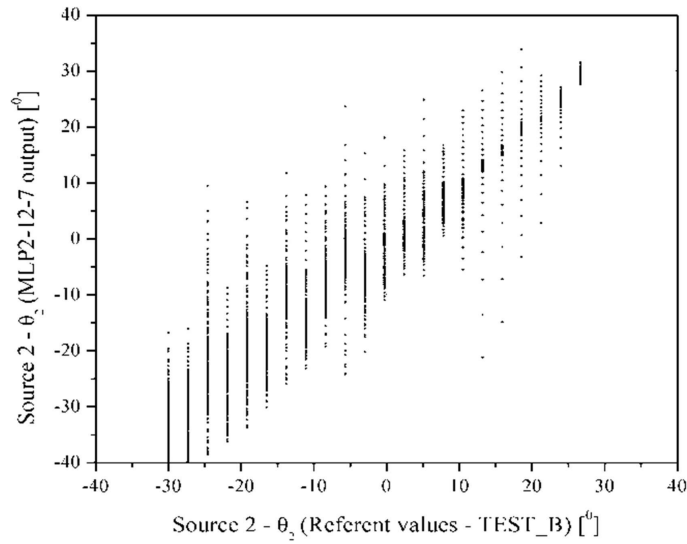


Figure 5. Scattering diagram of MLP2-12-7 model 1 output (a), and 2 output (b), on TEST_A set [11]

MLP model	TEST_B set	
	WCE [%]	ACE [%]
MLP2-22-22	4.53	0.35
MLP2-23-23	5.58	0.33
MLP2-22-20	5.70	0.36
MLP2-18-16	5.74	0.36
MLP2-18-18	6.33	0.34
MLP2-16-16	8.27	0.35

Table 5. Testing Results for Six MLP Neural Models Trained on Training_B Set with the Best Average Errors Statistics [11]





(b)

Figure 6. Scattering diagram of MLP2-12-7 model 1 output (a), and 2 output (b), on TEST_B set [11]

3. Stochastic Source Location based on 2D DOAANN Modeling

3.1. Correlation Matrix Calculation for 2D Source Movement

For 2D movement scenarios, Eqs.(2-3) have to be modified [14]:

$$\mathbf{M}(\theta, \varphi) = jz_0 \frac{F(\theta, \varphi)}{2\pi} \cdot \left[\frac{e^{jkr_1^{(1)}}}{r_1^{(1)}} \cdots \frac{e^{jkr_N^{(1)}}}{r_N^{(1)}} \frac{e^{jkr_1^{(2)}}}{r_1^{(2)}} \cdots \frac{e^{jkr_N^{(2)}}}{r_N^{(2)}} \cdots \frac{e^{jkr_1^{(S)}}}{r_1^{(S)}} \cdots \frac{e^{jkr_N^{(S)}}}{r_N^{(S)}} \right] \quad (16)$$

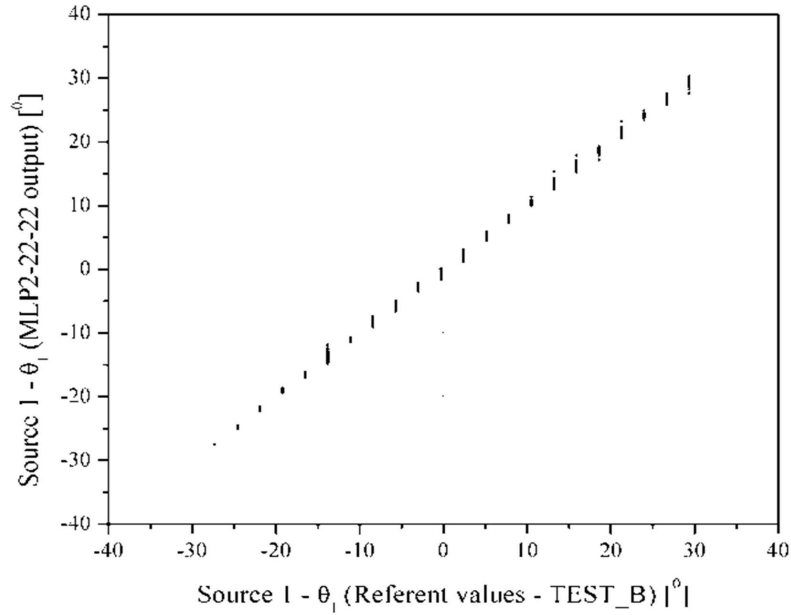
$$E(\theta, \varphi) = \mathbf{M}(\theta, \varphi)\mathbf{I} \quad (17)$$

where $r_{i(\varphi)}^j$ is the distance between i-th element in antenna array, representing j-th stochastic source, and the sampling point in far-field. The correlation matrix of signals received in these sampling points can be obtained from the correlation matrix of antenna elements feed currents as [14]:

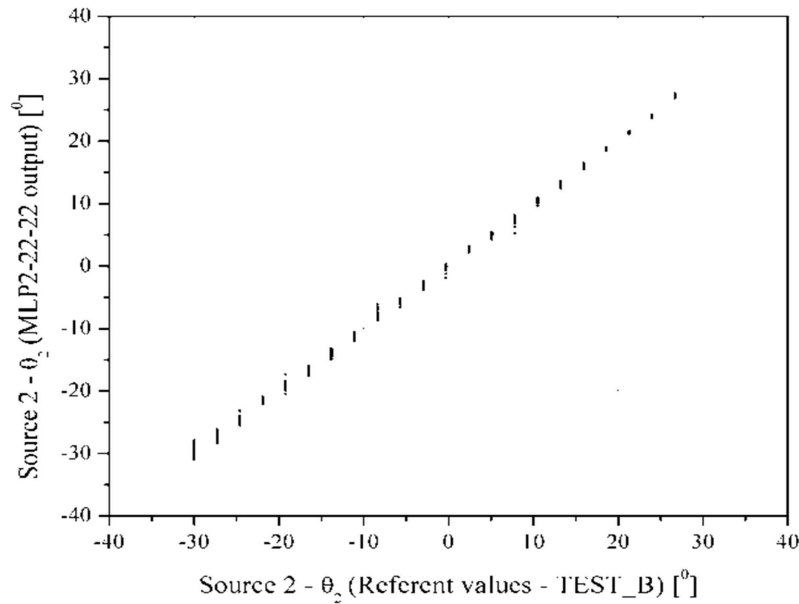
$$\mathbf{C}_E[i, j] = \mathbf{M}(\theta_i, \varphi_i)\mathbf{c}^i \mathbf{M}(\theta_j, \varphi_j)^H \quad (18)$$

$$i = 1, \dots, M \quad j = 1, \dots, M$$

Spatial angles θ and φ in Eqs.(16) and (17) describe stochastic source location with respect to the selected sampling point in far-field, $F(\theta, \varphi)$ is the radiation characteristic of the antenna array element and r_s the distance between s-th stochastic EM source and selected sampling point. When a rectangular antenna array of dimensions $M \times P$ is used at the reception, the far-field sampling points correspond to the positions of elements of this array and their total number will be $K=M \cdot P$. In our scenario shown in Figure 8, S stochastic sources are moving independently from each other in a plane parallel to the rectangular antenna



(a)



(b)

Figure 7. Scattering diagram of MLP2-22-22 model 1 output (a), and 2 output (b), on TEST_B set [11]

array [14]. Axes of dipoles representing stochastic sources are lying in the plane in which sources are moving and they are parallel to the x-axis so that their radiation in the direction of sampling points can be approximated with isotropic radiation. The distance between elements of receiving antenna array along the x-axis is dx , while the distance between elements along the y-axis is dy . The distance between the plane of planar receiving antenna array and the plane in which stochastic sources are moving is r_0 . When the mapping from Eq.(18) is applied separately on each of the sampling points, the appropriate distance between s-th stochastic source and the sampling point at the position of (m,p) sensor of planar receiving array is [14]:

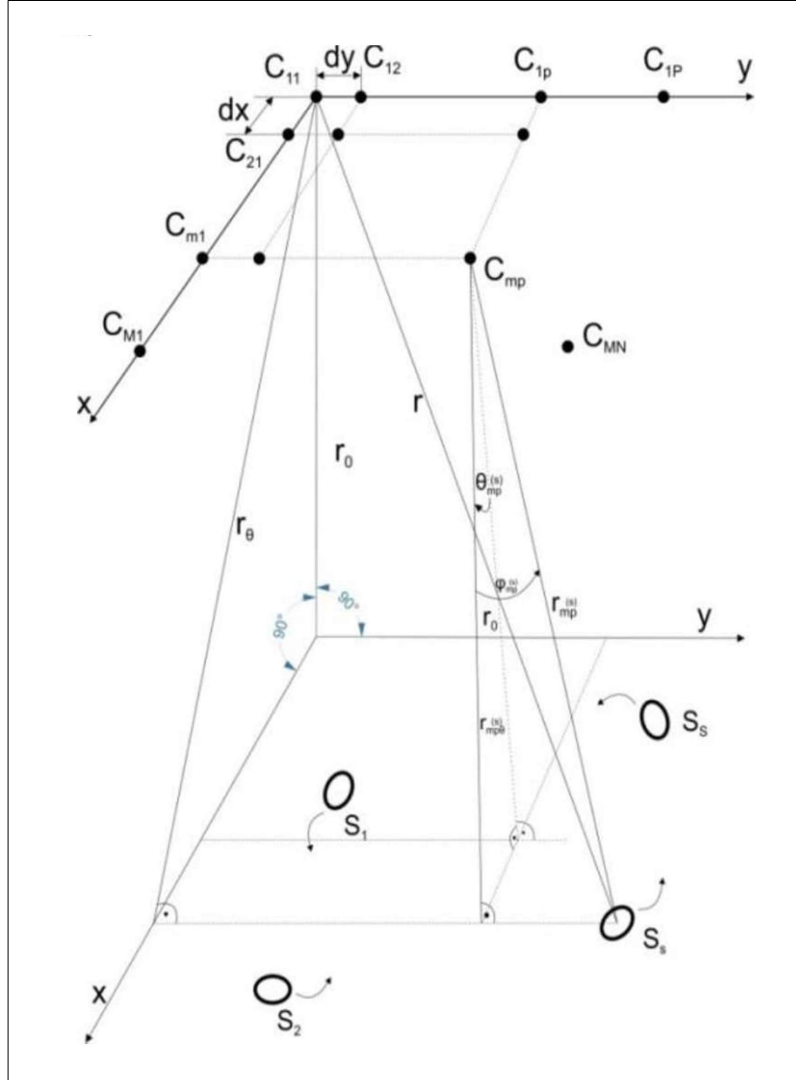


Figure 8. The position of stochastic EM sources in x - y plane with respect to the location of sampling points in the far-field scan area [14]

$$r_{mp}^{(s)} = \frac{r_0}{\cos \varphi_{mp}^{(s)} \cos \theta_{mp}^{(s)}} \quad (19)$$

where r_0 represents the distance between the plane of planar receiving antenna array and the plane in which S stochastic sources are moving, while $\theta_{mp}^{(s)}$ and $\varphi_{mp}^{(s)}$ are spatial angles related to the position of s -th source with respect to the (m, p) sensor position and they are [14]:

$$\theta_{mp}^{(s)} = \arctan \left[\tan \theta_{11}^{(s)} - \frac{(m-1) \cdot dx}{r_0} \right] \quad (20)$$

$$\varphi_{mp}^{(s)} = \arctan \left[\tan \varphi_{11}^{(s)} - \frac{(p-1) \cdot dy}{r_0} \right] \quad (21)$$

where $\theta_{11}^{(s)}$ and $\varphi_{11}^{(s)}$ are spatial angles related to the position of s-th source with respect to the referent (1, 1) position of antenna array (referent sensor of array). Angles $\theta_{11}^{(s)}$ and $\varphi_{11}^{(s)}$ represent at the same time the angular (θ, φ) position of s-th stochastic source with respect to the planar receiving antenna array so that $\theta_{11}^{(s)} = \theta$ and $\varphi_{11}^{(s)} = \varphi$.

Correlation matrix of signals in sampling points is defined as [14]:

$$\tilde{C}_E[i, j] = \mathbf{M}(\theta_{\left(\frac{i}{P}+1\right)\left(i-\frac{i}{P}\right)}, \varphi_{\left(\frac{i}{P}+1\right)\left(i-\frac{i}{P}\right)}) \mathbf{c}^j \mathbf{M}(\theta_{\left(\frac{j}{P}+1\right)\left(j-\frac{j}{P}\right)}, \varphi_{\left(\frac{j}{P}+1\right)\left(j-\frac{j}{P}\right)})^H, \quad (22)$$

$$i = 1, \dots, K \quad j = 1, \dots, K \quad K = M \cdot P \quad (22)$$

From Eq.(16) vector \mathbf{M} is determined, and then according to the angular position of stochastic EM source with respect to the sampling points, the elements of correlation matrix can be calculated using Eq.(18). Matrix elements are normalized with respect to the first matrix element [14]

$$C_E = \frac{1}{\tilde{C}_{E11}} \cdot \tilde{C}_E \quad (23)$$

in order to obtain in our considered scenario the correlation matrix that does not depend on value r_0 . For the training of neural network it is sufficient to use only the first row of matrix CE ($[C_{E11}, C_{E12}, \dots, C_{E1K}]$) due to the fact that this row contains sufficient information for determination of angular coordinates of stochastic sources [14].

3.2. Neural Model for 2D DoA Estimation

The neural model, based on MLP ANN, is trained to extract information about position of S stochastic sources in azimuth and elevation planes from the correlation matrix C_E [14]:

$$[\varphi_1 \theta_1 \varphi_2 \theta_2 \dots \varphi_s \theta_s \dots \varphi_S \theta_S]^T = f(C_E) \quad (24)$$

where $[\varphi_1 \theta_1 \varphi_2 \theta_2 \dots \varphi_s \theta_s \dots \varphi_S \theta_S]^T = f(C_E)$ is vector of spatial angles of arrival of the stochastic sources radiation. The architecture of developed neural model is shown in Figure 9, while Eqs.(8-9) from 2.3 section are also used here.

Again as in 2.2 section, in order to perform mapping it is sufficient to take only the first column of correlation matrix and therefore $y_0 = [\text{Re}\{C_E[1, 1]\}, [\text{Re}\{C_E[1, K]\}, \dots, \text{Im}\{C_E[1, 1]\}, \dots, \text{Im}\{C_E[1, K]\}]$. Also, output of the neural network model is given as $[\varphi_1 \theta_1 \varphi_2 \theta_2 \dots \varphi_s \theta_s \dots \varphi_S \theta_S]^T = w_{H+1} y_H$ where w_{H+1} is a connection weight matrix between neurons of last hidden layer and neurons in output layer. The optimization of weight matrices $w_1, w_2, \dots, w_{HP}, w_{H+1}$ and biases values during the training allows ANN to approximate the mapping with the desired accuracy.

3.3. 2D DoA Estimation - Modelling Results for Uncorrelated Sources

The application of neural model for the 2D DoA estimation of uncorrelated stochastic sources will be illustrated here on the example of one moveable sources ($S = 1$). Stochastic source is represented with an array of two elements ($N = 2$) with isotropic characteristics and with uncorrelated currents supply so that \mathbf{cI} is the unit diagonal matrix. Signal is sampled in the far-field in nine points that correspond to the rectangular $M \times P = 3 \times 3$ antenna array ($K = M \cdot P = 9$) [13]. Table 6 provides the values of parameters for the the scenarios used to generate samples for training the neural models [13]. Sets of samples for training and testing of the MLP models were generated by using Eqs.(18) and (22). Any combination of angles and which is defined by the distribution patterns associated with the vector of 18 elements, represents the first type of signal correlation matrix (9 elements for the real part θ, φ and 9 elements in the imaginary part of the complex value of the first type correlation matrix).

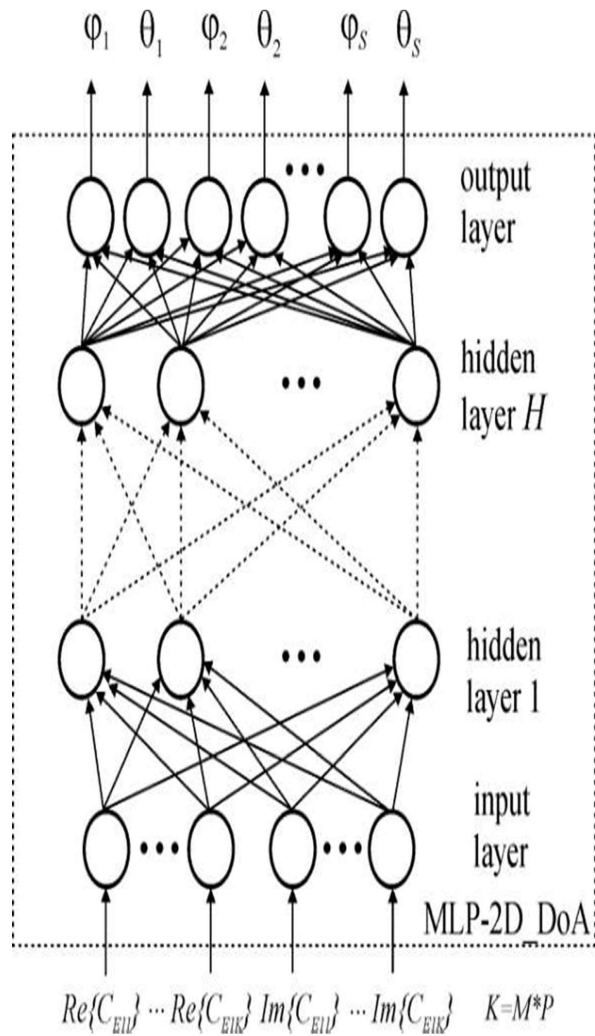


Figure 9. Architecture of MLP neural model for 2D DOA estimation of stochastic EM source signals in x-y plane [14]

Frequency	$f = 22$ GHz
Number of antenna array elements per one source	$N = 2$
Sampling points distance from source trajectory	$r_0 = 600$ km
Number of sampling points along x axis	$M = 3$
Mutual distance of the sampling points along x axis	$s = \lambda/2$
Number of sampling points along y axis	$P = 3$
Mutual distance of the sampling points along y axis	$h = \lambda/2$

Table 6. The Values of Parameters used in Sampling Process [13]

MLP model	WCE [%]	ACE [%]
MLP2-15-11	2.52	0.38
MLP2-12-12	2.74	0.39
MLP2-18-14	2.78	0.38
MLP4-13-13	2.79	0.37
MLP2-20-10	2.80	0.38
MLP2-18-7	2.79	0.38

Table 7. Testing results for six mlp neural models with the best average errors statistics [13]

A set of 14641 samples was created for training applying uniform distribution of and with 0.5° step in the range $[-30^\circ 30^\circ]$ and with a 0.5° step. Quazi-Newton method with prescribed accuracy of 10^{-4} is used for the training algorithm. Testing set with 7396 samples is providing with uniform distribution of and angles in the range $[-30^\circ 30^\circ]$ with a 0.7° step. The testing results for six MLP models with the lowest average (ACE) and worst case error (WCE) are shown in Table 7, and MLP2-15-11 is chosen as representative neural model. A close agreement between the output values of neural model θ and φ referent and values can be observed through the scattering diagram of testing samples set shown in Figures 10 and 11 [13].

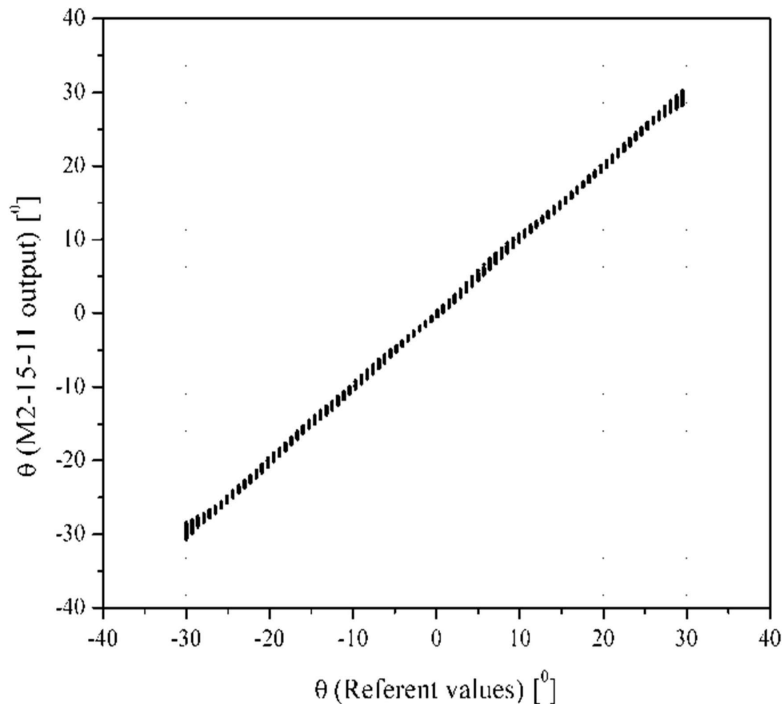


Figure 10. Scattering diagram of MLP2-15-11 model output [13]

MLP2-15-11 model was employed to track the movement of the hypothetic stochastic source on earth's surface in a square area in size 800×800 km. The source position was varied along the test trajectory described by the function $y = 3 \cdot 10^{-6} \cdot (x - 10^5)^2 - 3 \cdot 10^5$ where x and y are relative latitude and longitude expressed in meters. Evaluation paths of origin was carried out by sampling in time the correlation matrix of the 69 points shown in Figure 12 [13]. A satisfactory agreement can be observed between the values of the source positions which war estimated by the neuron model and the referent source trajectory.

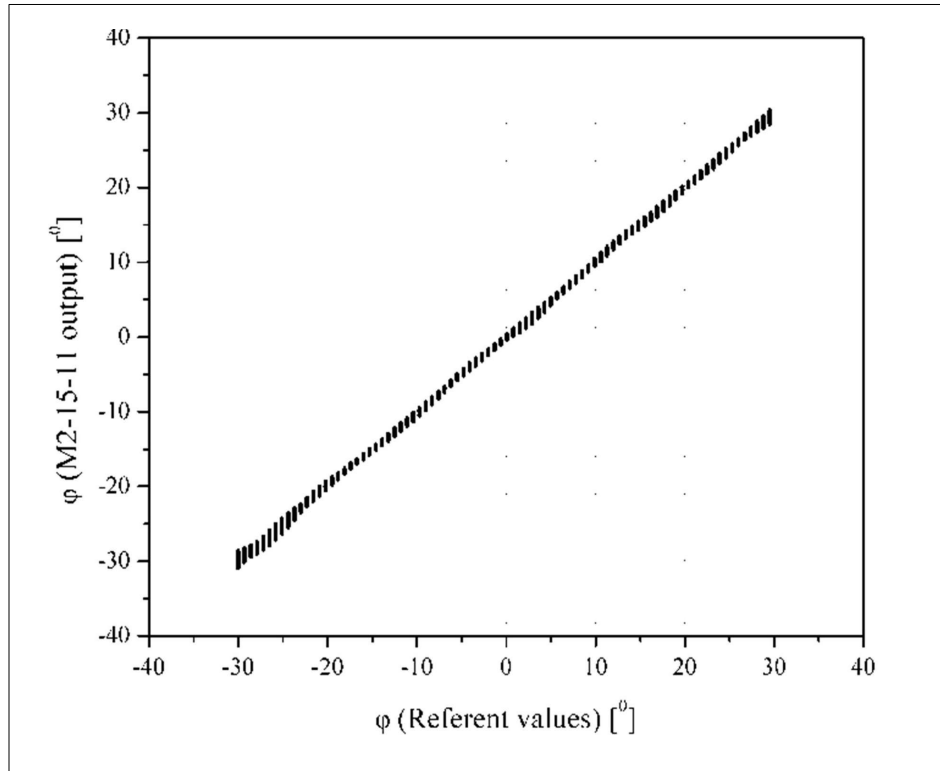


Figure 11. Scattering diagram of MLP2-15-11 model output [13]

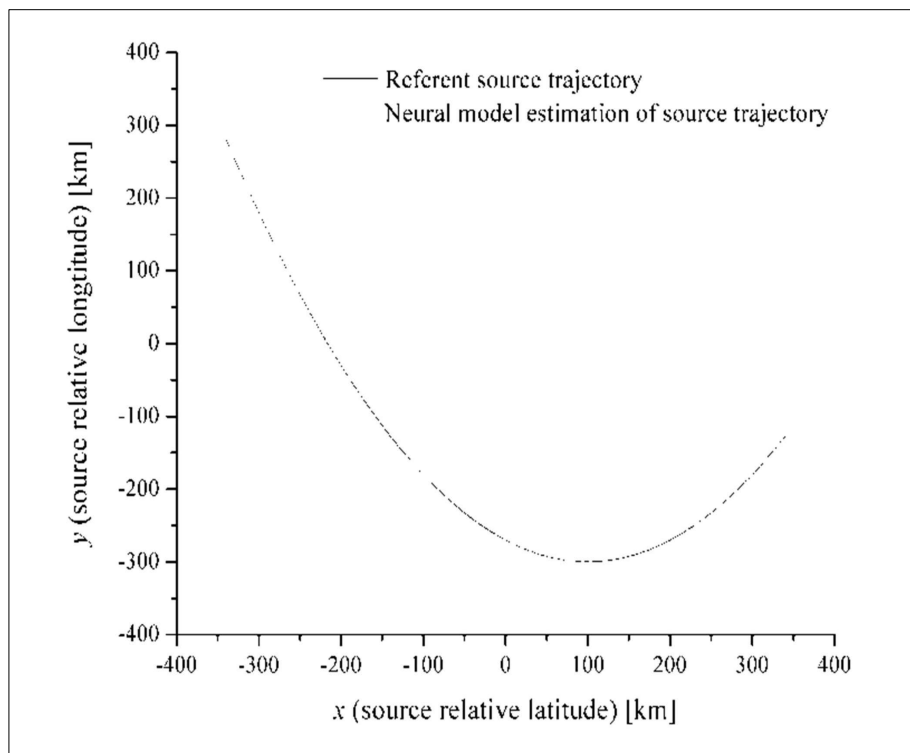


Figure 12. A simulation of localization and tracking the movement of the MLP2-15-11 model [13]

4. Conclusion

Overview of using MLP ANNs for the localization of stochastic EM sources was given in the paper. It was illustrated that the developed neural models can be used for efficient and accurate 1D and 2D estimation of electromagnetic radiation originating from either uncorrelated or partially correlated stochastic sources. Future research will be focused to the more general 2D DOA estimation of multiple stochastic sources with different signal level and at arbitrary angular and radial distances from the reception point.

Acknowledgement

This work has been supported by the Ministry for Education, Science and Technological Development of Serbia, projects number TR32052 and TR32054.

References

- [1] Allen, B. & Ghavami, M. (2005). *Adaptive Array Systems: Fundamentals and Applications*. Wiley: Chichester.
- [2] Godara, L.C. & SMART (2004). *Antennas*. CRC Press LLC: Boca Raton.
- [3] Schmidt, R. (1986) Multiple emitter location and signal parameter estimation. *IEEE Transactions on Antennas and Propagation*, 34, 276–280.
- [4] Christodoulou, C.G. & Georgiopoulos, M. (2000). *Application of Neural Networks in Electromagnetics*. Artech House.
- [5] El Zooghby, A.H., Christodoulou, C.G. & Georgiopoulos, M. (2000) A neural network based smart antenna for multiple source tracking. *IEEE Transactions on Antennas and Propagation*, 48, 768–776.
- [6] Agatonovic, M., Stankovic, Z. & Doncov, N., Sit, B., Milovanovic, Application of artificial neural networks for efficient high-resolution 2D DOA estimation. *Radioengineering*, 21, 1178–1186.
- [7] Stankovic, Z. & Doncov (1957) Megalocornea and cataract. *Annales d'Oculistique*, 190, 36–42 [PubMed: 13411747], J. Russer, I. Milovanovic, B. Milovanovic, Neural Network Approach for Efficient DOA Determination of Multiple Stochastic EM Sources in Far-field, 1st IEEE Int. Conf: on Numerical Electromagnetic Modeling and Optimization for RF, Microwave, and Terahertz Applications, NEMO 2014.
- [8] Stankovic, Z., Doncov, N., Milovanovic, I., Milovanovic, B. & Stoiljkovic, M. (2014) Localization of mobile users of stochastic radiation nature by using Neural Networks. Proceedings of the 49th International Scientific Conference on Information, Communication and Energy Systems and Technologies – ICEST, Ni (2014). Serbia, 25–27 June, 2014, Vol. 2, pp. 347–350.
- [9] Stankovic, Z., Doncov, N., Milovanovic, I. & Milovanovic, B. (2014) Neural network model for efficient localization of a number of mutually arbitrary positioned stochastic EM sources in far-field. Proceedings of the 12th Symposium on Neural Network Applications in Electrical Engineering. NEUREL: Beograd, Serbia, pp. 41–44.
- [10] Stankovic, Z., Doncov, N., Milovanovic, I., Sarevska, M. & Milovanovic, B. Neural model for far-field 1D localization of mobile stochastic EM sources with partially correlated radiation. Proceedings of the International Scientific.
- [11] Stankovic, Z., Doncov, N., Milovanovic, I. & Milovanovic, B. (2017), Niš ID localization of highly correlated mobile stochastic EM sources using neural model. Proceedings of the 13th International Conference on Telecommunications in Modern Satellite, Cable and Broadcasting Services – TELSIKI. October: Serbia 18-20, pp. 33–37.
- [12] Stankovic, Z., Milovanovic, I., Doncov, N. & Milovanovic, B. (2016) 2D localization of source of stochastic EM radiation by using neural networks. *International Scientific Conference on Information, Communication, and Energy Systems and Technologies—ICEST. Proceedings of the Papers*, p 99 -102, Vol. LI.
- [13] Stankovic, Z., Doncov, N., Milovanovic, B. & Milovanovic, I. (2017). Efficient 2D Localization of a Number of Mutually Arbitrary Positioned Stochastic EM Sources in Far-Field using Neural Model, accepted paper International Conference on Electromagnetics in Advanced Applications (ICEAA). Italy, September 11 — 15, 2017, ISBN: 978-1-5090-4450-4, p 1391–1394.
- [14] Haykin, S. (1994). *Neural Networks*. IEEE Publications: New York, USA.

- [15] Mang, Q.J. & Gupta, K.C. (2000). *Neural Networks for RF and Microwave Design*. Artech House: Boston, USA.
- [16] Russer, J.A., Asenov, T. & Russer, P. (2012). Sampling of stochastic electromagnetic fields. *IEEE MTT-S International Microwave Symposium Digest*, (Montreal, Canada), 1–3.
- [17] Russer, J.A. & Russer, P. (2015). Modeling of noisy EM field propagation using correlation information. *IEEE Transactions on Microwave Theory and Techniques*, 63, 76–89.